Environmental Science & Technology

Article

pubs.acs.org/est

Bioconcentration of Perfluorinated Alkyl Acids: How Important Is Specific Binding?

Carla A. Ng* and Konrad Hungerbühler

Institute for Chemical and Bioengineering, ETH Zurich, Wolfgang-Pauli-Strasse 10 CH-8093 Zurich, Switzerland

Supporting Information

ABSTRACT: Perfluorinated alkyl acids (PFAAs) are important global pollutants with unique pharmacokinetics. Evidence is accumulating that their behavior within organisms is affected by interaction with a number of proteins. In mammals, serum albumin, fatty acid binding proteins (FABPs) and organic anion transporters (OATs) have been identified as important to the tissue distribution, species-specific accumulation, and species- and gender-specific elimination rates of perfluoroalkyl carboxylates and perfluoroalkane sulfonates. Similar pharmacokinetics has been identified in fish. Yet, no mechanistic model exists for the bioaccumulation of PFAAs in fish that explicitly considers protein interactions. In this work, we present the first mechanistic protein-binding bioconcentration model for PFAAs in fish. Our model considers PFAA uptake via passive diffusion at the gills, association with serum albumin in the circulatory and extracellular spaces, association with FABP in the liver, and renal elimination and reabsorption facilitated by OAT proteins. The model is evaluated using measured bioconcentration and tissue distribution data collected in two previous studies of rainbow trout (*Oncorhynchus mykiss*) and common carp (*Cyprinus carpio*). Comparing our model with previous attempts to describe PFAA bioconcentration using a nonspecific (partitioning-type) approach shows that inclusion of protein interactions is key to accurately predicting tissue-specific PFAA distribution and bioconcentration.

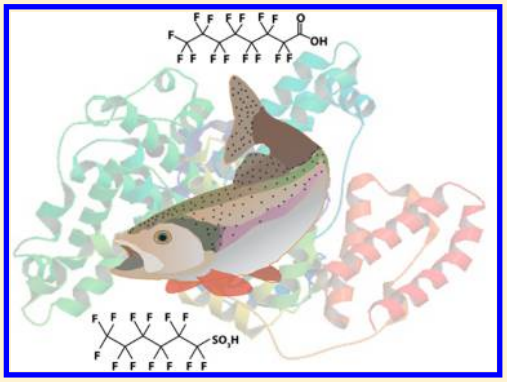

1. INTRODUCTION

Perfluorinated alkyl acids (PFAAs), including perfluoroalkyl carboxylic acids (PFCAs) and perfluoroalkane sulfonic acids (PFSAs) belong to an important class of highly persistent, bioaccumulative industrial chemicals detected on a global scale.[1−6]

Field and laboratory studies indicate that, in contrast to neutral hydrophobic contaminants, the blood plasma, liver, and kidney are key sites for PFAA accumulation.[7−10] Adipose and muscle are typically the compartments with lowest levels[4,8,11,12] (an exception is a recent study on Great Lakes herring gulls,[13] where adipose tissue had the highest concentrations of PFSAs but not PFCAs). Furthermore, PFAAs display substantial interspecies variability in tissue distribution and clearance rates.[7] For some PFAAs, gender-specific differences in elimination rates have been reported.[14−17]

PFAA toxicokinetics have been most well studied in mammals, where three important features of their uptake and disposition have been identified. First, PFAAs are strongly bound to albumin in the plasma,[18−20] making blood an important accumulation medium.[2,12,21−23] Second, PFAA transport into cells is most likely controlled by a combination of passive diffusion and facilitation by transporter proteins.[15,24] Organic anion transporter (OAT) proteins, like the human OAT4 and URAT-1 proteins, are renal transporters that facilitate the reabsorption of organic anions from urine back to blood, and are thought to be responsible for the long half-life of some PFAAs.[24] The rat ortholog to these proteins, Oatp1a1, is more highly expressed in males than in females and thus may explain the observed gender difference in rat PFOA clearance rates.[17] Third, PFAAs bind to cytosolic fatty acid binding proteins (FABPs), which are ubiquitous in a number of cell types, and thus serve as an important PFAA sink in certain tissues.[25−27]

Albumin, OATs and FABPs are all proteins active in fatty acid metabolism.[26,28−32] If we conclude from observations in mammals that proteins active in fatty acid metabolism influence PFAA accumulation, similar mechanisms may also affect PFAA bioaccumulation in fish. Many of the same proteins, or proteins having similar function, have been identified in fish. Albumin-like proteins are found in salmonids, including rainbow trout.[33] In carp, where no albumin has been identified, high-density lipoprotein (HDL) performs many of the same transport functions.[34] Orthologs to mammalian OATs and FABPs have been identified in a number of fish species.[30,35−43] In Atlantic salmon, fatty acid uptake by hepatocytes is mediated by both passive diffusion and a saturable, inhibitable protein-mediated uptake mechanism.[44] Finally, gender-specific differences in PFAA clearance rates in fathead minnow[16] and tissue-specific

Received: October 26, 2012
Revised: May 31, 2013
Accepted: June 4, 2013
Published: June 4, 2013

   dx.doi.org/10.1021/es400981a | Environ. Sci. Technol. 2013, 47, 7214−7223

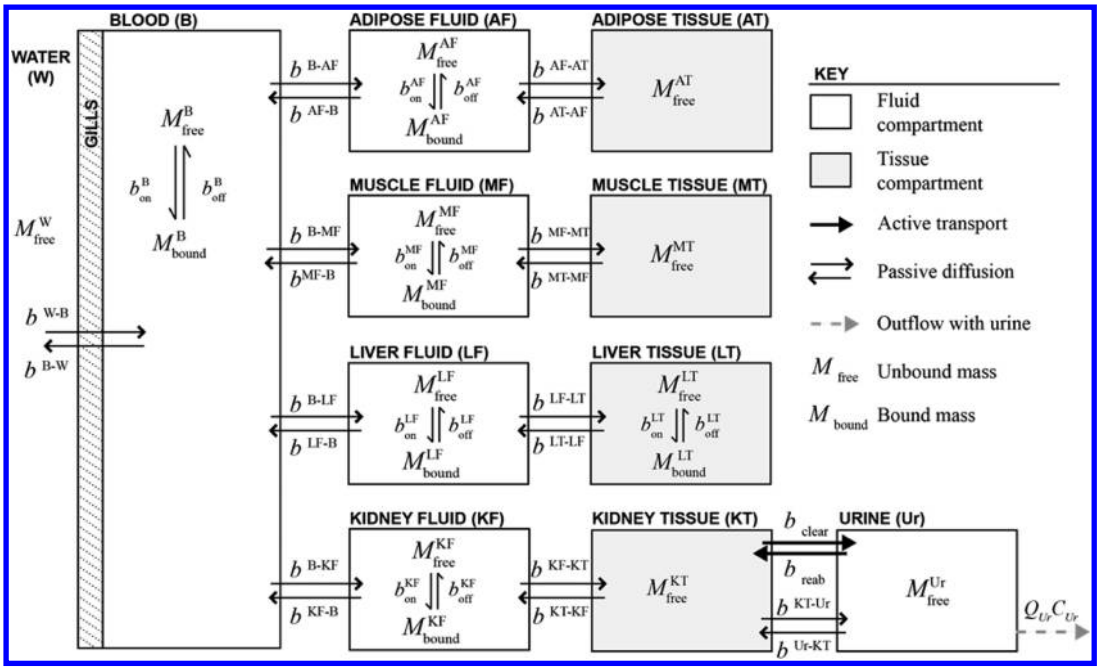

Figure 1. Model schematic indicating protein interactions in blood (B), interstitial fluid (AF, MF, LF, KF) and liver tissue (LT) compartments. Intercompartment exchange occurs via passive diffusion (all compartments) and active renal clearance (b_{clear}) and reabsorption (b_{reab}) facilitated by OAT proteins in kidney tissue (KT).

bioaccumulation in male and female zebrafish[45] indicate that some interactions between PFAAs and fatty acid transporters are conserved from mammals to fish. Yet, only one study to date has specifically addressed PFAA−protein interactions in fish.[46] No mechanistic models exist to assess the impact of protein interactions on PFAA accumulation in fish.

In this work, we construct a novel protein-binding model for the bioconcentration of PFAAs in fish. The model explicitly considers binding of PFAAs to serum albumin in blood and interstitial fluids, binding to FABP in the liver, and renal clearance facilitated by organic anion transporters (OATs). Given the lack of fish-specific data, the model utilizes all available protein interaction data collected for a variety of species, primarily mammals. We test whether the bioaccumulation patterns the model predicts are consistent with what has been measured in bioconcentration experiments with rainbow trout (*Oncorhynchus mykiss*)[11] and common carp (*Cyprinus carpio*).[47] The performance of our model is also discussed in the context of the only other models currently available for bioconcentration of PFAAs in fish: namely, the models of Webster and Ellis (2011)[48] and Armitage et al. (2013),[49] which both take an equilibrium partitioning approach.

2. MATERIALS AND METHODS

2.1. Model Structure. The model consists of 10 compartments (Figure 1): blood (B), adipose interstitial fluid (AF), adipose tissue (AT), muscle interstitial fluid (MF), muscle tissue (MT), liver interstitial fluid (LF), liver tissue (LT), kidney interstitial fluid (KF), kidney tissue (KT), and urine (Ur). The blood and interstitial fluid (extracellular) compartments contain albumin and thus PFAA−albumin binding can occur in these five compartments. The liver tissue compartment contains liver fatty acid binding protein (FABP) and thus PFAA−FABP binding can occur in this compartment.

PFAAs bind to albumin with rate constant b_{on} and dissociate with rate constant b_{off}. The kinetics are defined by the albumin equilibrium association constant, K_A^{Alb}, as described in Section 2.2, below. Within the liver tissue, PFAAs bind to and dissociate from liver fatty acid binding proteins (FABP) according to the equilibrium association constant, K_A^{FABP}.

Facilitated transport is included in the kidneys, where we model two competing protein-mediated processes: PFAA removal from the kidneys to urine (with rate constant b_{clear}) and reabsorption from the urine back to the kidneys (with rate constant b_{reab}). For transport between any other pair of compartments, i and j, we consider passive diffusion only, with rate constant b^{i-j}. Passive diffusion is possible only for free (unbound) PFAA. Clearance occurs by advection with urine (with rate $Q_{Ur}C_{Ur}$) or via passive diffusion at the gills (with rate constant b^{B-W}).

Because no data are available for PFAA fecal egestion, it is currently not included in our model. The relative importance of renal to fecal excretion of PFAAs is unknown in fish. In mice and rats PFCAs are eliminated in urine and only much more slowly in feces.[50,51] For longer-chained PFCAs (C9 and greater), where renal excretion is low, fecal excretion may be more important.[50]

2.2. Rate Constants for Protein Interactions. To describe binding to albumin (Alb) or to liver fatty acid binding protein (FABP), we utilize published equilibrium association constants (K_A^{Alb} or K_A^{FABP}, respectively). These equilibrium constants are ratios of individual association and dissociation rate constants.[19,20,52−56]

$$K_A^P = k_{on}^P / k_{off}^P \quad (1)$$

The association rate constant for a protein p, k_{on}^p, is a second-order rate constant in units of $M^{-1}s^{-1}$, because the association rate it describes depends both on the mass of substrate (PFAA) that is binding to the protein and on the concentration of available binding sites.[57,58] The dissociation rate constant, on the other hand, is a first-order rate constant in units of s^{-1}, and is multiplied by the mass of bound PFAA to determine the

dx.doi.org/10.1021/es400981a | Environ. Sci. Technol. 2013, 47, 7214−7223

Table 1. PFAA Mass Balances

	mass balance[a]
blood (B)[b]	$\frac{dM^{B}_{free}}{dt} = b^{W-B}C^{W}_{free} - b^{B-W}M^{B}_{free} - \sum_i b^{B-iF}M^{B}_{free} + \sum_i b^{iF-B}M^{iF}_{free} - b^{B}_{on}M^{B}_{free} + b^{B}_{off}M^{B}_{bound}$
	$\frac{dM^{B}_{bound}}{dt} = b^{B}_{on}M^{B}_{free} - b^{B}_{off}M^{B}_{bound}$
adipose fluid (AF)	$\frac{dM^{AF}_{free}}{dt} = b^{B-AF}M^{B}_{free} + b^{AT-AF}M^{AT}_{free} - (b^{AF-B} + b^{AF-AT})M^{AF}_{free} - b^{AF}_{on}M^{AF}_{free} + b^{AF}_{off}M^{AF}_{bound}$
	$\frac{dM^{AF}_{bound}}{dt} = b^{AF}_{on}M^{AF}_{free} - b^{AF}_{off}M^{AF}_{bound}$
adipose tissue (AT)	$\frac{dM^{AT}_{free}}{dt} = b^{AF-AT}M^{AF}_{free} - b^{AT-AF}M^{AT}_{free}$
muscle fluid (MF)	$\frac{dM^{MF}_{free}}{dt} = b^{B-MF}M^{B}_{free} + b^{MT-MF}M^{MT}_{free} - (b^{MF-B} + b^{MF-MT})M^{MF}_{free} - b^{MF}_{on}M^{MF}_{free} + b^{MF}_{off}M^{MF}_{bound}$
	$\frac{dM^{MF}_{bound}}{dt} = b^{MF}_{on}M^{MF}_{free} - b^{MF}_{off}M^{MF}_{bound}$
muscle tissue (MT)	$\frac{dM^{MT}_{free}}{dt} = b^{MF-MT}M^{MF}_{free} - b^{MT-MF}M^{MT}_{free}$
liver fluid (LF)	$\frac{dM^{LF}_{free}}{dt} = b^{B-LF}M^{B}_{free} + b^{LT-LF}M^{LT}_{free} - (b^{LF-B} + b^{LF-LT})M^{LF}_{free} - b^{LF}_{on}M^{LF}_{free} + b^{LF}_{off}M^{LF}_{bound}$
	$\frac{dM^{LF}_{bound}}{dt} = b^{LF}_{on}M^{LF}_{free} - b^{LF}_{off}M^{LF}_{bound}$
liver tissue (LT)	$\frac{dM^{free}_{LT}}{dt} = b^{LF-LT}M^{LF}_{free} - b^{LT-LF}M^{LT}_{free} - b^{LT}_{on}M^{LT}_{free} + b^{LT}_{off}M^{LT}_{bound}$
	$\frac{dM^{LT}_{bound}}{dt} = b^{LT}_{on}M^{LT}_{free} - b^{LT}_{off}M^{LT}_{bound}$
kidney fluid (KF)	$\frac{dM^{KF}_{free}}{dt} = b^{B-KF}M^{B}_{free} + b^{KT-KF}M^{KT}_{free} - (b^{KF-B} + b^{KF-KT})M^{KF}_{free} - b^{KF}_{on}M^{KF}_{free} + b^{KF}_{off}M^{KF}_{bound}$
	$\frac{dM^{iF}_{bound}}{dt} = b^{KF}_{on}M^{KF}_{free} - b^{KF}_{off}M^{KF}_{bound}$
kidney tissue (KT)	$\frac{dM^{KT}_{free}}{dt} = b^{KF-KT}M^{KF}_{free} - (b^{KT-KF} + b^{KT-Ur})M^{KT}_{free} + b^{Ur-KT}M^{Ur}_{free} - b_{clear}M^{KT}_{free} + b_{reab}M^{Ur}_{free}$
urine (Ur)	$\frac{dM^{Ur}_{free}}{dt} = b^{KT-Ur}M^{KT}_{free} - b^{Ur-KT}M^{Ur}_{free} + b_{clear}M^{KT}_{free} - b_{reab}M^{Ur}_{free} - \frac{Q_{Ur}}{V^{Ur}}M^{Ur}_{free}$

[a] M_{free} refers to unbound PFAA, which is free to move between compartments, while M_{bound} is chemical bound to albumin or, in the liver tissue, FABP. [b] In summation expressions, i = A (adipose), M (muscle), L (liver), and K (kidney).

dissociation rate in units of mol/s. The concentration of available binding sites in relevant compartments is calculated through six population balances: for blood, liver fluid, liver tissue, kidney fluid, muscle fluid, and adipose fluid. All take the general form

$$\frac{dc_p^{i,unocc}}{dt} = k^p_{off}C^i_{bound} - k^p_{on}C_p^{i,unocc}C^i_{free} \quad (2)$$

$C_p^{i,unocc}$ is the concentration of available (unoccupied) binding sites of protein p in compartment i. The dissociation rate constant for protein p is k^p_{off}, and the association rate constant is k^p_{on}. The concentration of PFAA bound to protein in compartment i is C^i_{bound} and the concentration of free PFAA is C^i_{free} In each of these balances, the initial concentration of available binding sites in a compartment is the total concentration of protein in the compartment multiplied by the number of binding sites per protein molecule, which can be PFAA-specific (see Table 2).

Using the concentration of available binding sites we can calculate a PFAA binding rate constant in compartment i, b^i_{on}, in units of s^{-1}:

dx.doi.org/10.1021/es400981a | Environ. Sci. Technol. 2013, 47, 7214−7223

Table 2. Summary of Association Constants (K_A) and Binding Sites (n) for PFAA Binding to Albumin (Alb) and Fatty Acid Binding Protein (FABP), with Their Sources

	K_A^{Alb} (M^{-1})		source		K_A^{FABP} (M^{-1})	source
	low	high	low	high		
PFOA	3.7×10^3 (n = 7.5)	1.4×10^6 (n = 1.4)	Han (2003)[52]	Bischel (2010)[54]	5.6×10^4 (n = 1)[a]	Woodcroft (2010)[56]
PFDA	4.7×10^4 (n = 2.3)	4.4×10^5 (n = 1)[a]	Hebert (2010)[19]	Qin (2010)[53]	6.4×10^5 (n = 1)[a,b]	〃
PFUnA	4.3×10^4 (n = 2.4)	3.0×10^5 (n = 1)[a]	〃	MacManus-Spencer (2010)[20]	2.2×10^6 (n = 1)[a,b]	〃
PFDoA		1.2×10^6 (n = 1)[a]		Chen (2009)[18]	7.4×10^6 (n = 1)[a,b]	〃
PFHxS	1.2×10^4 (n = 1.65)		Hebert (2010)[19]		1.7×10^4 (n = 1)[a,b]	〃
PFOS	8.9×10^3 (n = 2.1)	7.6×10^6 (n = 1)[a]	〃	Chen (2009)[18]	1.9×10^5 (n = 1)[a,b]	〃

[a]Value refers to primary binding site. [b]Woodcroft et al. (2010) provide values for C5−C9 PFCAs. We use their data to extrapolate values for all our PFAAs as explained in SI Section S3-4.

$$b_{on}^{i} = k_{on}^{p} C_{p}^{i,unocc} \quad (3)$$

The PFAA dissociation rate constant in compartment i, b_{off}^{i}, is the first order dissociation rate constant for protein p, k_{off}^{p}, with units of s^{-1}:

$$b_{off}^{i} = k_{off}^{p} \quad (4)$$

Only the equilibrium constant, K_A^p, is available from literature. No studies currently exist that specifically measure the individual association and dissociation rate constants (k_{on}^{p} and k_{off}^{p}) for PFAAs with either albumin or FABPs. However, in this work we focus on the steady-state results, which depend only on K_A^p and on the total concentration of protein p in compartment i, C_p^i, but not on the individual association and dissociation constants, as shown in the Supporting Information (SI) (Section S4-2).

2.3. PFAA Mass Balance Equations. In addition to the protein site balances, there are 16 PFAA mass balances that describe the PFAA−protein interactions and exchange between each of the model compartments depicted in Figure 1: there are two for blood (one for free chemical and one for chemical bound to albumin); two each for the liver, kidney, muscle, and adipose interstitial fluid compartments (for free and albumin-bound chemical); one each for the muscle and adipose tissue compartments, where no binding occurs; two for the liver tissue compartment (one for free chemical and one for chemical bound to FABP); one for the kidney tissue compartment and finally one for urine. These mass balances are listed in Table 1. A glossary of all model parameters is provided in the SI (Section S1). All first-order rate constants for transport among compartments are described in detail in the SI, Sections S3-2 and S4-1.

2.4. Model Parameterization. *Fish Physiology.* Our model represents a generic 8 g fish (similar to the size of rainbow trout used in the experiment of Martin et al. (2003)),[11] for which we need corresponding compartment volumes (V^i), areas for intercompartment exchange (A^{i-j}), albumin concentrations in blood serum and interstitial fluid compartments (C_{Alb}^{i}) and an estimate of the FABP concentration in liver tissue (C_{FABP}^{LT}).

In SI section S2-1 we explain how compartment volumes are derived using the work of Barron et al. (1987), Gingerich et al. (1987) and Bushnell et al. (1988).[59−61] Compartment volumes are summarized in SI Tables S1 and S2. Areas for intercompartment exchange are estimated by assuming a simplified capillary geometry and scaled according to organ-specific blood volumes, based on the work of Soldatov (2006) and Gingerich et al. (1987),[60,62] as detailed in SI Section S2-1 and summarized in Table S3. In SI Section S2-3 we describe how blood, water and urine flow rates were estimated for our 8-g fish. These values are summarized in SI Table S4.

Albumin concentrations are estimated based on both fish and mammalian literature. Manera and Britti[33] provide an estimate of C_{Alb}^{B} for rainbow trout serum. For the interstitial fluid compartments, no fish-specific data were available. However, a study on human subjects provided estimates of concentrations in muscle and adipose interstitial fluid relative to serum levels;[63] additional mammalian studies have shown that albumin concentrations in interstitial fluids of the liver are about half that in plasma, and we assume a similar level for the kidney.[28,64] We assume tissue compartments contain no albumin. Finally, we estimate the concentration of FABP in liver tissues as approximately 50 μM, following Londraville (1996).[65] All protein concentrations used in the model are summarized in SI Table S5.

PFAA Properties. We consider six PFAAs for which sufficient bioconcentration and protein interaction data exist to assess our model performance: perfluorooctanoic acid (PFOA), perfluorodecanoic acid (PFDA), perfluoroundecanoic acid (PFUnA), perfluorododecanoic acid (PFDoA), perfluorohexane sulfonate (PFHxS), and perfluorooctane sulfonate (PFOS). Their structures are shown in SI Figure S2.

For uptake from water to blood, we use measured passive PFAA diffusion rates in different types of cells.[15,17,24] From these rates we calculate effective membrane permeabilities for each PFAA, which are then used to calculate the rate constants for passive diffusion to and from the blood via the gills (b^{W-B} and b^{B-W}, respectively, see SI Sections S3-2 and S4-1 for details).

Two types of protein interaction data are needed: binding and transport. The model uses equilibrium association constants to describe binding to albumin in the blood and interstitial fluid compartments (K_A^{Alb}), and to FABPs in the liver tissue compartment (K_A^{FABP}). In the kidney tissue, rate constants are needed to describe clearance (b_{clear}) and reabsorption (b_{reab}) via OAT-facilitated transport.

For the equilibrium association constant with albumin (K_A^{Alb}), data are largely restricted to interactions with bovine and human serum albumin. We compile data from five recent studies: Han et al. (2003),[52] Chen et al. (2009),[18] Hebert et al. (2010),[19] MacManus-Spencer et al. (2010),[20] Bischel et al. (2010),[54] and Qin et al. (2010).[53] From these studies, which estimated K_A^{Alb} using a variety of techniques, we extract the minimum (low) and maximum (high) values reported for six PFAAs (Table 2). Most of the low values are found in the Hebert et al. (2010) study, which uses fluorescence spectroscopy, whereas Bischel et al. (2010), using equilibrium dialysis, and Chen et al. (2009), who used site-specific fluorescence,

provide the highest values. In the case of PFHxS and PFDoA, only one binding constant for each was available. For PFHxS the value is from the Hebert et al. (2010) study; we assume this is a lower bound. For PFDoA, the value from the Chen et al. (2009) study is among the highest reported for any PFAA. We assume this to represent a higher-end estimate.

Although FABPs are ubiquitous in many tissues and have been identified in zebrafish,[40] striped bass,[42] Atlantic salmon,[30,39] and rainbow trout,[41] no data are currently available for association constants of PFAAs with FABPs in fish. The interactions of C5−C9 PFAAs with FABPs have been measured in rat hepatocytes by Woodcroft et al. (2010).[56] We use their study to extrapolate equilibrium binding constants between PFAAs and FABPs in the liver for C8−C12 PFCAs and assume PFSA−FABP binding strengths are equal to those for PFCAs of equivalent perfluorinated carbon chain length (see SI Section S3-4).

Fatty acid transport proteins, of which OATs are a class, have been identified as active in fatty acid transport in fish heart, adipose, brain, gills, and intestine.[35,39] However, data for PFAA interaction with these transporter proteins are completely lacking for fish and in the mammalian literature are largely restricted to hepatocyte uptake[15] or renal transport.[17,24] Of these studies, only the renal OAT study by Weaver et al. (2010)[17] considers multiple PFAAs. We thus derive rate constants for facilitated clearance and reabsorption in the kidney using the Weaver et al. study, as described in SI Section S3-3 and Table S7.

2.5. Model Assessment. In all, the model includes 35 independent parameters (SI Tables S9 and S10). However, there are no fitted parameters. Due to lack of data for PFAA−protein interactions in fish, many of these values are based on literature studies for mammals (primarily rats and humans). Thus a favorable comparison between our model results and measured tissue distribution and bioconcentration data for fish is not only an assessment of our model, but also of the plausibility of parallels in PFAA-protein interactions between mammals and fish. In section S3-5 and Table S8 of the SI we discuss the species-specific origin of protein parameters used in the model. We also perform a sensitivity analysis (SI Section S5) to identify all parameters to which our model is most sensitive.

3. RESULTS

3.1. Tissue Distributions. We first compare the tissue distributions predicted by our model to the data from Martin et al. (2003)[11] (Figure 2) for PFOA, PFDA, PFUnA, PFDoA, PFHxS, and PFOS. In order to predict concentrations for comparison with these data, we ran the model for each PFAA using the exposure concentration given by Martin et al. In their paper, they note PFDoA concentrations in water were below the limit of detection (LOD) of 0.4 μg/L, and in their Table 1 list the water concentration of PFDoA as 0.2 μg/L, or 1/2 the limit of detection. In our model runs, we take both values (0.2 and 0.4 μg/L) and show the predicted range in Figure 2 using a dotted line.

Where more than one value for the equilibrium association constant with albumin (K_A^{Alb}) was available for a single PFAA, we show the range of predictions obtained using the lowest and highest values (Figure 2, black lines). The height of the bar indicates the average between low and high predictions where two K_A^{Alb} values were available or the single value predicted when only one K_A^{Alb} was available.

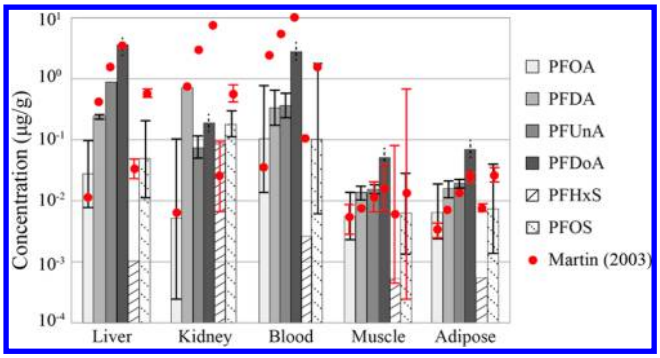

Figure 2. PFAA tissue distribution. Model predictions (bars) and values measured by Martin et al. (2003)[11] (red circles, one standard error indicated by red line). Prediction ranges for PFOA, PFDA, PFUnA, and PFOS based on reported K_A^{Alb} ranges (see Table 2) are indicated by black lines. The black dotted line for PFDoA predictions is based on exposure concentrations of 0.2 and 0.4 μg/L (1/2 the limit of detection and the limit of detection in the Martin et al. study, respectively).

Two features can be assessed here: the distribution of PFAAs across different compartments, and the concentrations of different PFAAs in each compartment. The tissue distribution predicted by our model (blood ≈ liver > kidney > muscle ≈ adipose) is similar to that measured by Martin et al. (blood > liver ≈ kidney > muscle ≈ adipose). However, our model generally under-predicts levels in the kidney and blood and overpredicts them (to a smaller extent) in adipose. In all compartments except the kidney the model-predicted mean concentrations follow the same chain length dependence as the data for the PFCAs: PFDoA > PFUnA > PFOA. For the PFSAs, the model correctly predicts that PFOS > PFHxS, but because PFHxS is under-predicted in liver, blood and adipose compartments, they do not show the same PFCA to PFSA pattern as the data.

In the liver compartment, for which we include both albumin and FABP interactions, values for all PFAAs are within a factor of 2 of measured concentrations, except for PFHxS, which is underestimated by a factor of 20. For PFOA and PFDoA, the measured concentration lies within the prediction range.

In the kidney, predictions for PFDA and PFOS are within a factor of 1.5, and both PFOA and PFHxS measured concentrations overlap our prediction ranges. However, the model substantially underestimates concentrations for PFUnA and PFDoA, one of the largest deviations observed (a factor of 25). Furthermore, the distribution in the kidney compartment does not follow the same pattern as the other compartments. This is due to the effect of competing clearance and reabsorption processes, which also follow a chain-length-dependence but not in a uniform way (for example, reabsorption increases with chain length more rapidly than clearance).[17]

In the blood compartment, both PFOS and PFOA data are within the prediction range. PFDoA and PFDA are both underestimated but within a factor of 4 of the measured data. PFUnA, on the other hand, is underestimated by nearly an order of magnitude, and PFHxS by a factor of 30.

In the muscle compartment, all prediction ranges except for PFDA fall within the range of measured values, and PFDA is overestimated by only about a factor of 1.4. Finally, predictions for the adipose compartment are all within about a factor of 1.5

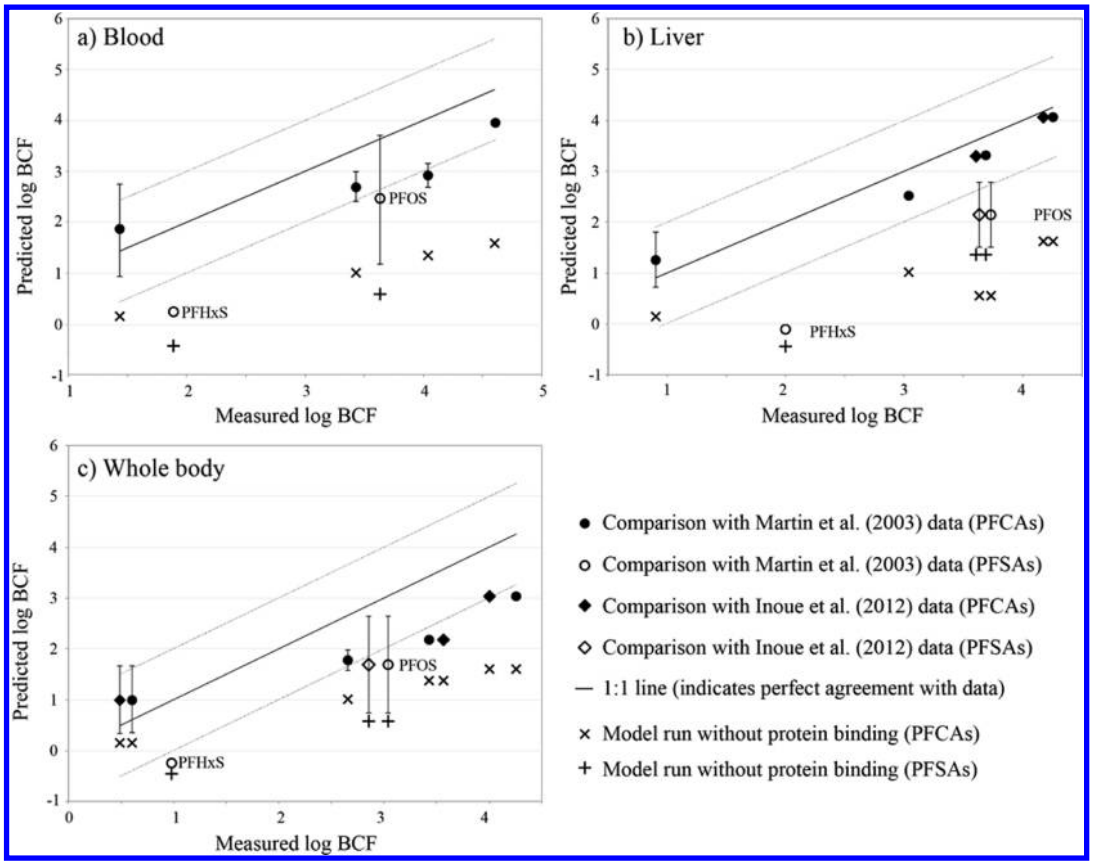

Figure 3. Comparison of predicted and measured bioconcentration factors (BCF) for PFCAs (solid symbols) and PFSAs (hollow symbols) in (a) blood, (b) liver, and (c) whole body. Ranges are indicated for predictions derived using low and high values for the albumin association constant (K_A^{Alb}). Solid line is 1:1 line indicating perfect agreement with data; dotted lines indicate ±1 log unit. Data are from Martin et al. (2003)[11] (circles) and Inoue et al. (2012)[47] (diamonds). Model predictions without considering specific protein binding are also shown (× for PFCAs, + for PFSAs).

of the measured data except for PFHxS, which is under-predicted by a factor of 11.

A clear strength of our model is the ability to predict PFAA concentrations well within an order of magnitude across different compartments that are characterized as having both a high degree of protein interaction (e.g., liver, blood) and relatively little protein interaction (muscle, adipose). However, PFHxS is substantially under-predicted in liver, muscle and adipose compartments. As noted in the section on PFAA properties, we expect the single value for K_A^{Alb} available for this chemical is likely a lower bound. In the kidney compartment, the PFAA distribution pattern predicted by our model was not observed in the rainbow trout data of Martin et al. (2003)[11] and there were large deviations for PFUnA and PFDoA concentrations. Thus, it is likely that the active clearance and reabsorption processes we modeled based on rat data do not operate in the same way or to the same extent in fish.

3.2. Tissue-Specific Bioconcentration Factors. We next evaluate our model performance in predicting PFAA bioconcentration factors (BCF). In this case, because the BCF relates the concentration in the tissue to that in the surrounding water, we run all model calculations assuming the same concentration in water (1×10^{-6} mol/m^3). We compare our predictions to data for rainbow trout from Martin et al. (2003)[11] and common carp from Inoue et al. (2012).[47]

For rainbow trout, BCF data were available for carcass (which Martin et al. suggest are within 80−90% of a whole body value), blood and liver. In common carp, data were available for whole body, viscera, integument, and "remaining parts".[47] We compare rainbow trout blood data to model predictions for the blood compartment. We compare rainbow trout liver and common carp viscera data to model predictions for the liver compartment. For the whole body BCF, we sum the steady-state mass of PFAAs predicted by our model over all of our compartments and divide by the exposure concentration. We compare this to rainbow trout carcass and common carp whole body data.

In cases where a range of K_A^{Alb} values was used, a range of predicted BCFs is indicated. In addition, we plot the predictions of our model with binding to albumin and FABP removed to illustrate the model run with only nonspecific (passive diffusion) interactions considered (Figure 3).

Predicted BCFs (Figure 3) are within one log unit of measured BCFs in all compartments and for every PFAA considered except for PFHxS and, in the whole body compartment, PFUnA (both Martin et al. and Inoue et al. data sets) and PFDoA (Martin et al. data set only). PFHxS is under-predicted in all compartments, by a factor of 20 in the whole body (where the least overall binding is expected due to inclusion of the muscle and adipose compartments) and a factor of 130 in the liver (where the most binding—to both albumin and FABP—is included).

In the blood compartment (Figure 3a), the range of predicted BCFs for PFOA and PFOS encompasses the measured data. The model-predicted BCF of PFDA is within a factor of 3 of the data, the BCF of PFDoA is within a factor of 4, and the predicted BCF of PFUnA is within a factor of 8.

In the liver compartment (Figure 3b), the predicted BCF range of PFOA encompasses the measured data. The BCFs of PFDA, PFUnA and PFDoA are all within a factor of 3 of the measured BCFs. The model-data agreement is by far the best in the liver compartment, where both albumin and FABP binding are included in the model.

Measured PFOA BCFs from both the Martin et al. and Inoue et al. data sets are within the range of predicted whole-body BCFs (Figure 3c). The predicted BCF of PFOS is within a factor of 3 of the measured data. As stated above, the predicted BCFs of PFUnA, PFDoA (for the Martin et al. data set), and PFHxS fall outside a factor of 10 of the data. In general the model under-predicts BCFs in the whole body.

For all three BCFs (blood, liver and whole body), when the model is run without protein binding none of the predictions for any PFAA are within a factor of 10 of the measured data. The only exception is PFOA in the whole body and the liver. Most BCFs are under-predicted by close to 2 log units, or a factor of 100. Thus the inclusion of protein binding is essential to the predictive power of the model.

3.3. Sensitivity Analysis. In order to probe the effect of parameter uncertainties on model predictions, we performed a factor-at-a-time sensitivity analysis over all independent model parameters (see SI Section S5). The analysis revealed that out of the 35 independent model parameters, most important are the equilibrium association constants for binding to albumin (K_A^{Alb}) and the availability of binding sites, as described by the concentration of albumin in a given compartment (C^i_{Alb}) and the number of binding sites per albumin molecule (n). Second most important are parameters related to passive diffusion at the gills, namely the effective membrane permeability (P_{eff}), the steady-state concentration ratio (CR_{SS}^{C-W}) that describes the back-diffusion mass transfer coefficient (see SI Section S3-2) and the area for blood-water exchange (A^{B-W}, the gill area). Finally, the ratio of interstitial fluid to tissue subcompartment volumes, though less important than either the binding or the diffusion parameters, affects predictions of compartment-specific BCFs.

4. DISCUSSION

The tissue distributions and bioconcentration factors predicted by our model are in good agreement with observations in rainbow trout and common carp, except for the substantial under-estimation of PFHxS. Model performance is best in the liver, which is also the most well characterized compartment in terms of protein binding, since both albumin and liver FABP binding data were available.[18−20,52−54,56] Model performance is also good in the blood, where the albumin concentration, and thus the fraction of bound PFAA, is highest. Like the liver, the blood compartment is relatively well characterized; there was a trout-specific measured concentration of albumin available,[33] and K_A^{Alb} values for all modeled PFAAs (see Table 2).

Model performance was not as strong in the whole body, where PFAA BCFs were generally under-predicted. This may be explained by the lack of FABP binding in other compartments where no data were available, although it is known that other fish tissues also contain FABPs.[42] The model also relies on empirical estimates of membrane permeability and includes active uptake only in the kidney; it is possible that either passive diffusion was under-predicted or that active uptake should be included in more compartments.

The most poorly predicted PFAA, in all compartments, was PFHxS. As previously noted, only one value of K_A^{Alb} for PFHxS was available from the literature,[19] and we expect that this value represents a lower bound. The general pattern observed in the data suggests that sulfonic acids behave differently from carboxylic acids and that their protein binding strengths may be stronger than indicated by their perfluorinated carbon chain lengths. The measured BCFs of PFOS in all compartments are between those of PFDA and PFUnA, whereas PFOS has the same number of perfluorinated carbons as PFNA. This is further supported by the high value of K_A^{Alb} estimated for PFOS,[18] which gives the best BCF predictions in our model. Similarly, the measured BCF of PFHxS is consistently higher than that of PFOA, despite PFOA having an additional perfluorinated carbon. If this pattern follows for all protein interactions, higher binding strengths with FABPs, which have not yet been measured for PFSAs, should be expected.

This work is the first fish bioconcentration model that explicitly considers PFAA−protein interactions. Only two other fish-specific PFAA bioconcentration models have been published to date. The first, by Webster and Ellis (2010),[48] is a partitioning-based model that assumes that only the neutral fraction of the chemical is available for uptake. They argue that equilibrium partitioning is sufficient to explain whole-body BCF values for PFAAs, based on an assumed pK_a for perfluorinated acids of 3.8 and using the K_{OW} of the neutral fraction (adjusted by the fraction of neutral chemical at biological pH) to predict the BCF. However, the weight of evidence from current research points to a pK_a value for most PFCAs of about 1.0 or lower.[66−69] Using this more realistic value, their model would under-predict PFAA BCFs by several orders of magnitude. Our model, which has a much higher degree of biological fidelity and does not rely on such assumptions about the physicochemical properties of PFAAs, can successfully predict the amount and tissue-specific distribution of these chemicals in fish.

More recently, Armitage et al. (2013) developed a bioconcentration model for ionizable organic chemicals in fish.[49] It focuses on two parameters: an octanol−water distribution coefficient, D_{OW}, for interaction of both neutral and charged species with neutral (storage) lipids, and a membrane−water distribution coefficient D_{MW}, which characterizes the interaction of both neutral and ionized species with membrane phospholipids. Because of the partially charged nature of phospholipids, the D_{MW} does not decrease as rapidly with degree of ionization as the D_{OW} and thus the model can help to explain higher than expected accumulation of ionizable compounds in fish. The authors apply this model to a number of PFAAs. However, results are only compared to the Martin et al. (2003) carcass BCFs, and no information is given for how the model might be parametrized for other organs. Given that blood serum and liver are important for PFAA accumulation,[8,9,13] the performance of a PFAA bioconcentration model for these compartments is key. Although we agree that nonspecific membrane partitioning may play a part in PFAA accumulation, our model results illustrate that it cannot provide the full picture.

Our model includes some important features that have not previously been implemented in fish bioconcentration models. These include PFAA interactions with albumin in serum and interstitial fluid compartments and with FABPs in the liver tissue. The inclusion of active renal clearance and reabsorption driven by interactions with OATs led to a mismatch between our model predictions in the kidney and available tissue distribution data. This suggests that renal transport may not be

as important in fish as it is in mammals, or that active transport rates differ substantially from mammals to fish. The lack of agreement for this particular compartment reinforces the need for fish-specific studies of protein interactions. To date, the work of Jones et al. (2003)[46] is the only one that looks at the interaction of PFAAs with fish serum proteins. However, the overall success of our model to predict patterns of tissue distribution and bioconcentration in both trout and carp suggests that parallels do exist between fish and mammalian systems in the way proteins interact with PFAAs. Given that our model is based on parameters measured for a variety of species and that there are no fitted parameters, the agreement between model predictions and measured data seems remarkable.

The wide ranges found in the literature for values of K_A^{Alb} for single PFAAs indicate that uncertainty in binding strength is still high. Given the importance of these parameters, as highlighted by our sensitivity analysis, more comprehensive studies are needed to measure protein interactions for a wider range of proteins and PFAAs at environmentally relevant PFAA concentrations. Importantly, different techniques lead to substantially different estimates; more systematic testing of these techniques is warranted.

Our model holds promise for the prediction of tissue-specific bioconcentration in fish, and may be useful as a tool to investigate further gaps in our knowledge regarding how these important chemicals operate within organisms. Of particular importance is the move by industry away from long-chain PFAAs. Not only are shorter-chain PFAAs being produced in increasing amounts, but the diversity of structures is also increasing. If the bioaccumulation potential of PFAAs is tied to their similarities with fatty acids, will that similarity hold for different structures such as branched chemicals? Can bulkier molecules occupy the same hydrophobic pockets exploited by fatty acids and linear perfluoroalkyl acids,[70] or do protein interactions with branched structures differ in important ways? Further protein interaction and bioaccumulation studies on different perfluorinated structures are clearly needed.

■ ASSOCIATED CONTENT

Supporting Information

Details of model parametrization and a model sensitivity analysis are available in the Supporting Information (SI). This material is available free of charge via the Internet at http://pubs.acs.org.

■ AUTHOR INFORMATION

Corresponding Author

*E-mail: carla.ng@chem.ethz.ch.

Notes

The authors declare no competing financial interest.

■ REFERENCES

(1) Martin, J.; Whittle, D.; Muir, D.; Mabury, S. Perfluoroalkyl contaminants in a food web from Lake Ontario. *Environ. Sci. Technol.* **2004**, *38*, 5379−5385.

(2) Houde, M.; Martin, J.; Letcher, R.; Solomon, K.; Muir, D. Biological monitoring of polyfluoroalkyl substances: A review. *Environ. Sci. Technol.* **2006**, *40*, 3463−3473.

(3) Kärrman, A.; Langlois, I.; Bavel, B.; Lindström, G.; Oehme, M. Identification and pattern of perfluorooctane sulfonate (PFOS) isomers in human serum and plasma. *Environ. Int.* **2007**, *33*, 782−788.

(4) Conder, J. M.; Hoke, R. A.; Wolf, W.; Russell, M. H.; Buck, R. C. Are PFCAs bioaccumulative? A critical review and comparison with regulatory criteria and persistent lipophilic compounds. *Environ. Sci. Technol.* **2008**, *42*, 995−1003.

(5) Schenker, U.; Scheringer, M.; Macleod, M.; Martin, J. W.; Cousins, I. T.; Hungerbühler, K. Contribution of volatile precursor substances to the flux of perfluorooctanoate to the Arctic. *Environ. Sci. Technol.* **2008**, *42*, 3710−3716.

(6) Kannan, K. Perfluoroalkyl and polyfluoroalkyl substances: Current and future perspectives. *Environ. Chem.* **2011**, *8*, 333−338.

(7) Verreault, J.; Houde, M.; Gabrielsen, G. W.; Berger, U.; Haukås, M.; Letcher, R. J.; Muir, D. C. G. Perfluorinated alkyl substances in plasma, liver, brain, and eggs of glaucous gulls (*Larus hyperboreus*) from the Norwegian Arctic. *Environ. Sci. Technol.* **2005**, *39*, 7439−7445.

(8) Ahrens, L.; Siebert, U.; Ebinghaus, R. Total body burden and tissue distribution of polyfluorinated compounds in harbor seals (*Phoca vitulina*) from the German Bight. *Mar. Pollut. Bull.* **2009**, *58*, 520−525.

(9) Yoo, H.; Guruge, K. S.; Yamanaka, N.; Sato, C.; Mikami, O.; Miyazaki, S.; Yamashita, N.; Giesy, J. P. Depuration kinetics and tissue disposition of PFOA and PFOS in white leghorn chickens (*Gallus gallus*) administered by subcutaneous implantation. *Ecotox. Environ. Safe.* **2009**, *72*, 26−36.

(10) Vestergren, R.; Cousins, I. T. Tracking the pathways of human exposure to perfluorocarboxylates. *Environ. Sci. Technol.* **2009**, *43*, 5565−5575.

(11) Martin, J.; Mabury, S.; Solomon, K.; Muir, D. Bioconcentration and tissue distribution of perfluorinated acids in rainbow trout (*Oncorhynchus mykiss*). *Environ. Toxicol. Chem.* **2003**, *22*, 196−204.

(12) Shi, Y.; Wang, J.; Pan, Y.; Cai, Y. Tissue distribution of perfluorinated compounds in farmed freshwater fish and human exposure by consumption. *Environ. Toxicol. Chem.* **2012**, *31*, 717−723.

(13) Gebbink, W. A.; Letcher, R. J. Comparative tissue and body compartment accumulation and maternal transfer to eggs of perfluoroalkyl sulfonates and carboxylates in Great Lakes herring gulls. *Environ. Pollut.* **2012**, *162*, 40−47.

(14) Ohmori, K.; Kudo, N.; Katayama, K.; Kawashima, Y. Comparison of the toxicokinetics between perfluorocarboxylic acids with different carbon chain length. *Toxicology* **2003**, *184*, 135−140.

(15) Han, X.; Yang, C.-H.; Snajdr, S. I.; Nabb, D. L.; Mingoia, R. T. Uptake of perfluorooctanoate in freshly isolated hepatocytes from male and female rats. *Toxicol. Lett.* **2008**, *181*, 81−86.

(16) Lee, J. J.; Schultz, I. R. Sex differences in the uptake and disposition of perfluorooctanoic acid in fathead minnows after oral dosing. *Environ. Sci. Technol.* **2009**, *44*, 491−496.

(17) Weaver, Y. M.; Ehresman, D. J.; Butenhoff, J. L.; Hagenbuch, B. Roles of rat renal organic anion transporters in transporting perfluorinated carboxylates with different chain lengths. *Toxicol. Sci.* **2010**, *113*, 305−314.

(18) Chen, Y.; Guo, L. Fluorescence study on site-specific binding of perfluoroalkyl acids to human serum albumin. *Arch. Toxicol.* **2009**, *83*, 255−261.

(19) Hebert, P.; Macmanus-Spencer, L. A. Development of a fluorescence model for the binding of medium- to long-chain perfluoroalkyl acids to human serum albumin through a mechanistic evaluation of spectroscopic evidence. *Anal. Chem.* **2010**, *82*, 6463−6471.

(20) Macmanus-Spencer, L. A.; Tse, M. L.; Hebert, P. C.; Bischel, H. N.; Luthy, R. G. Binding of perfluorocarboxylates to serum albumin: A comparison of analytical methods. *Anal. Chem.* **2010**, *82*, 974−981.

(21) Taniyasu, S.; Kannan, K.; Horii, Y.; Hanari, N.; Yamashita, N. A survey of perfluorooctane sulfonate and related perfluorinated organic compounds in water, fish, birds, and humans from Japan. *Environ. Sci. Technol.* **2003**, *37*, 2634−2639.

(22) Ankley, G.; Kuehl, D.; Kahl, M.; Jensen, K.; Linnum, A.; Leino, R.; Villeneuve, D. Reproductive and developmental toxicity and bioconcentration of perfluorooctanesulfonate in a partial life-cycle test

with the fathead minnow (*Pimephales promelas*). *Environ. Toxicol. Chem.* **2005**, *24*, 2316−2324.
(23) Kelly, B. C.; Ikonomou, M. G.; Blair, J. D.; Surridge, B.; Hoover, D.; Grace, R.; Gobas, F. A. P. C. Perfluoroalkyl contaminants in an Arctic marine food web: Trophic magnification and wildlife exposure. *Environ. Sci. Technol.* **2009**, *43*, 4037−4043.
(24) Yang, C.-H.; Glover, K. P.; Han, X. Characterization of cellular uptake of perfluorooctanoate via organic anion-transporting polypeptide 1A2, organic anion transporter 4, and urate transporter 1 for their potential roles in mediating human renal reabsorption of perfluorocarboxylates. *Toxicol. Sci.* **2010**, *117*, 294−302.
(25) Luebker, D. J.; Hansen, K. J.; Bass, N. M.; Butenhoff, J. L.; Seacat, A. M. Interactions of fluorochemicals with rat liver fatty acid-binding protein. *Toxicology* **2002**, *176*, 175−185.
(26) Weisiger, R. A. Mechanisms of intracellular fatty acid transport: Role of cytoplasmic-binding proteins. *J. Mol. Neurosci.* **2007**, *33*, 42−44.
(27) Hickey, N. J.; Crump, D.; Jones, S. P.; Kennedy, S. W. Effects of 18 perfluoroalkyl compounds on mRNA expression in chicken embryo hepatocyte cultures. *Toxicol. Sci.* **2009**, *111*, 311−320.
(28) Peters Jr., T. *All about Albumin: Biochemistry, Genetics, And Medical Applications*; Academic Press: New York, 1995.
(29) Van Der Vusse, G. J. Albumin as fatty acid transporter. *Drug Metab. Pharmacokinet.* **2009**, *24*, 300−307.
(30) Jordal, A.-E. O.; Hordvik, I.; Pelsers, M.; Bernlohr, D. A.; Torstensen, B. E. FABP3 and FABP10 in Atlantic salmon (*Salmo salar L.*)-General effects of dietary fatty acid composition and life cycle variations. *Comp. Biochem. Phys. B* **2006**, *145*, 147−158.
(31) Ahn, S.-Y.; Nigam, S. K. Toward a systems level understanding of organic anion and other multispecific drug transporters: A remote sensing and signaling hypothesis. *Mol. Pharmacol.* **2009**, *76*, 481−490.
(32) Riedmaier, A. E.; Nies, A. T.; Schaeffeler, E.; Schwab, M. Organic anion transporters and their implications in pharmacotherapy. *Pharmacol. Rev.* **2012**, *64*, 421−449.
(33) Manera, M.; Britti, D. Assessment of blood chemistry normal ranges in rainbow trout. *J. Fish Biol.* **2006**, *69*, 1427−1434.
(34) De Smet, H.; Blust, R.; Moens, L. Absence of albumin in the plasma of the common carp *Cyprinus carpio*: Binding of fatty acids to high density lipoprotein. *Fish Physiol. Biochem.* **1998**, *19*, 71−81.
(35) Popovic, M.; Zaja, R.; Smital, T. Organic anion transporting polypeptides (OATP) in zebrafish (*Danio rerio*): Phylogenetic analysis and tissue distribution. *Comp. Biochem. Phys. A* **2010**, *155*, 327−335.
(36) Aslamkhan, A. G.; Thompson, D. M.; Perry, J. L.; Bleasby, K.; Wolff, N. A.; Barros, S.; Miller, D. S.; Pritchard, J. B. The flounder organic anion transporter fOat has sequence, function, and substrate specificity similarity to both mammalian Oat1 and Oat3. *Am. J. Physiol.: Regul., Integr. Comp. Physiol.* **2006**, *291*, R1773−R1780.
(37) Meier-Abt, F.; Hammann-Hänni, A.; Stieger, B.; Ballatori, N.; Boyer, J. The organic anion transport polypeptide 1d1 (Oatp1d1) mediates hepatocellular uptake of phalloidin and microcystin into skate liver. *Toxicol. Appl. Pharmacol.* **2007**, *218*, 274−279.
(38) Boaru, D. A.; Dragoş, N.; Schirmer, K. Microcystin-LR induced cellular effects in mammalian and fish primary hepatocyte cultures and cell lines: A comparative study. *Toxicology* **2006**, *218*, 134−148.
(39) Torstensen, B.; Nanton, D.; Olsvik, P.; Sundvold, H.; Stubhaug, I. Gene expression of fatty acid-binding proteins, fatty acid transport proteins (cd36 and FATP) and β-oxidation-related genes in Atlantic salmon (*Salmo salar L.*) fed fish oil or vegetable oil. *Aquacult. Nutr.* **2009**, *15*, 440−451.
(40) Liu, R.; Denovan - Wright, E. M.; Wright, J. M. Structure, linkage mapping and expression of the heart-type fatty acid-binding protein gene (fabp3) from zebrafish (*Danio rerio*). *Eur. J. Biochem.* **2003**, *270*, 3223−3234.
(41) Ando, S.; Xue, X.-H.; Tibbits, G. F.; Haunerland, N. H. Cloning and sequencing of complementary DNA for fatty acid binding protein from rainbow trout heart. *Comp. Biochem. Phys. B* **1998**, *119*, 213−217.
(42) Londraville, R. L.; Sidell, B. D. Cold acclimation increases fatty acid-binding protein concentration in aerobic muscle of striped bass, *Morone saxatilis*. *J. Exp. Zool.* **1996**, *275*, 36−44.
(43) Di Pietro, S. M.; Dell'Angelica, E. C.; Veerkamp, J. H.; Sterin-Speziale, N.; Santomé, J. A. Amino acid sequence, binding properties and evolutionary relationships of the basic liver fatty-acid-binding protein from the catfish *Rhamdia sapo*. *Eur. J. Biochem.* **1997**, *249*, 510−517.
(44) Zhou, J.; Stubhaug, I.; Torstensen, B. E. Trans-membrane uptake and intracellular metabolism of fatty acids in Atlantic salmon (*Salmo salar L.*) hepatocytes. *Lipids* **2010**, *45*, 301−311.
(45) Zhang, W.; Zhang, Y.; Zhang, H.; Wang, J.; Cui, R.; Dai, J. Sex differences in transcriptional expression of FABPs in zebrafish liver after chronic perfluorononanoic acid exposure. *Environ. Sci. Technol.* **2012**, *46*, 5175−5182.
(46) Jones, P.; Hu, W.; De, C., W; Newsted, J.; Giesy, J. Binding of perfluorinated fatty acids to serum proteins. *Environ. Toxicol. Chem.* **2003**, *22*, 2639−2649.
(47) Inoue, Y.; Hashizume, N.; Yakata, N.; Murakami, H.; Suzuki, Y.; Kikushima, E.; Otsuka, M. Unique physicochemical properties of perfluorinated compounds and their bioconcentration in common carp *Cyprinus carpio L. Arch. Environ. Con. Tox.* **2012**, *62*, 672−680.
(48) Webster, E.; Ellis, D. Equilibrium modeling: A pathway to understanding observed perfluorocarboxylic and perfluorosulfonic acid behavior. *Environ. Toxicol. Chem.* **2011**, *30*, 2229−2236.
(49) Armitage, J.; Arnot, J.; Wania, F.; Mackay, D. Development and evaluation of a mechanistic bioconcentration model for ionogenic organic chemicals in fish. *Environ. Toxicol. Chem.* **2013**, *32*, 115−128.
(50) Kudo, N.; Suzuki, E.; Katakura, M.; Ohmori, K.; Noshiro, R.; Kawashima, Y. Comparison of the elimination between perfluorinated fatty acids with different carbon chain length in rats. *Chem. Biol. Interact.* **2001**, *134*, 203−216.
(51) Gannon, S.; Johnson, T.; Nabb, D.; Serex, T.; Buck, R.; Loveless, S. Absorption, distribution, metabolism, and excretion of [14C]-perfluorohexanoate ([14C]-PFHx) in rats and mice. *Toxicology* **2011**, *283*, 55−62.
(52) Han, X.; Snow, T. A.; Kemper, R. A.; Jepson, G. W. Binding of perfluorooctanoic acid to rat and human plasma proteins. *Chem. Res. Toxicol.* **2003**, *16*, 775−781.
(53) Qin, P.; Liu, R.; Pan, X.; Fang, X.; Mou, Y. Impact of carbon chain length on binding of perfluoroalkyl acids to bovine serum albumin determined by spectroscopic methods. *J. Agric. Food Chem.* **2010**, *58*, 5561−5567.
(54) Bischel, H.; Macmanus-Spencer, L. A.; Luthy, R. Noncovalent interactions of long-chain perfluoroalkyl acids with serum albumin. *Environ. Sci. Technol.* **2010**, *44*, 5263−5269.
(55) Han, X.; Nabb, D. L.; Russell, M. H.; Kennedy, G.; Rickard, R. Renal elimination of perfluorocarboxylates (PFCAs). *Chem. Res. Toxicol.* **2012**, *25*, 35−46.
(56) Woodcroft, M.; Ellis, D.; Rafferty, S.; Burns, D.; March, R.; Stock, N.; Trumpour, K.; Yee, J.; Munro, K. Experimental characterization of the mechanism of perfluorocarboxylic acids' liver protein bioaccumulation: The key role of the neutral species. *Environ. Toxicol. Chem.* **2010**, *29*, 1669−1677.
(57) Foy, B.; Frazier, J. Incorporation of protein-binding kinetics and carrier-mediated membrane transport into a model of chemical kinetics in the isolated perfused rat liver. *Toxicol. Mech. Methods* **2003**, *13*, 53−75.
(58) Robinson, P.; Rapoport, S. Kinetics of protein-binding determine rates of uptake of drugs by brain. *Am. J. Physiol.* **1986**, *251*, R1212−R1220.
(59) Barron, M.; Tarr, B.; Hayton, W. Temperature-dependence of cardiac output and regional blood flow in rainbow trout *Salmo gairdneri* Richardson. *J. Fish Biol.* **1987**, *31*, 735−744.
(60) Gingerich, W.; Pityer, R.; Rach, J. Estimates of plasma, packed cell and total blood-volume in tissues of the rainbow-trout (*Salmo gairdneri*). *Comp. Biochem. Phys. A* **1987**, *87*, 251−256.
(61) Bushnell, P. G.; Conklin, D. J.; Duff, D.; Olson, K. Tissue and whole-body extracellular, red blood cell and albumin spaces in the rainbow trout as a function of time: A reappraisal of the volume of the secondary circulation. *J. Exp. Biol.* **1998**, *201*, 1381−1391.

(62) Soldatov, A. Organ blood flow and vessels of microcirculatory bed in fish. *J. Evol. Biochem. Physiol.* **2006**, *42*, 243−252.
(63) Ellmerer, M.; Schaupp, L.; Brunner, G. A.; Sendlhofer, G.; Wutte, A.; Wach, P.; Pieber, T. R. Measurement of interstitial albumin in human skeletal muscle and adipose tissue by open-flow microperfusion. *Am. J. Physiol.: Endocrinol. Metab.* **2000**, *278*, E352−E356.
(64) Levitt, D. The pharmacokinetics of the interstitial space in humans. *BMC Clin. Pharmacol.* **2003**, *3*, 3.
(65) Londraville, R. Intracellular fatty acid-binding proteins: Putting lower vertebrates in perspective. *Braz. J. Med. Biol. Res.* **1996**, *29*, 707.
(66) Moroi, Y.; Yano, H.; Shibata, O.; Yonemitsu, T. Determination of acidity constants of perfluoroalkanoic acids. *Bull. Chem. Soc. Jpn.* **2001**, *74*, 667−672.
(67) López-Fontán, J. L.; Sarmiento, F.; Schulz, P. C. The aggregation of sodium perfluorooctanoate in water. *Colloid Polym. Sci.* **2005**, *283*, 862−871.
(68) Goss, K. U. The pKa values of PFOA and other highly fluorinated carboxylic acids. *Environ. Sci. Technol.* **2008**, *42*, 456−458.
(69) Cheng, J.; Psillakis, E.; Hoffmann, M.; Colussi, A. Acid dissociation versus molecular association of perfluoroalkyl oxoacids: Environmental implications. *J. Phys. Chem. A* **2009**, *113*, 8152−8156.
(70) D'Eon, J. C.; Simpson, A.; Kumar, R.; Baer, A.; Mabury, S. Determining the molecular interactions of perfluorinated carboxylic acids with human sera and isolated human serum albumin using nuclear magnetic resonance spectroscopy. *Environ. Toxicol. Chem.* **2010**, *29*, 1678−1688.